

## ATRP of Amphiphilic Graft Copolymers Based on PVDF and Their Use as Membrane Additives

J. F. Hester,<sup>†</sup> P. Banerjee, Y.-Y. Won, A. Akthakul, M. H. Acar, and A. M. Mayes\*

Department of Materials Science and Engineering, Massachusetts Institute of Technology,  
77 Massachusetts Avenue, Cambridge, Massachusetts 02139

Received December 21, 2001; Revised Manuscript Received July 3, 2002

**ABSTRACT:** The direct preparation of amphiphilic graft copolymers from commercial poly(vinylidene fluoride) (PVDF) using atom transfer radical polymerization (ATRP) is demonstrated. Here, direct initiation of the secondary fluorinated site of PVDF facilitates grafting of the hydrophilic comonomer. Amphiphilic comb copolymer derivatives of PVDF having poly(methacrylic acid) side chains (PVDF-*g*-PMAA) and poly(oxyethylene methacrylate) side chains (PVDF-*g*-POEM) are prepared using this method. Surface segregation of PVDF-*g*-POEM additives in PVDF is examined as a route to wettable, foul-resistant surfaces on PVDF filtration membranes. Because of surface segregation during the standard immersion precipitation process for membrane fabrication, a PVDF/5 wt % PVDF-*g*-POEM membrane, having a bulk POEM concentration of 3.4 wt %, exhibits a near-surface POEM concentration of 42 wt % as measured by X-ray photoelectron spectroscopy (XPS). This membrane displays substantial resistance to BSA fouling compared with pure PVDF and wets spontaneously when placed in contact with water.

### Introduction

Graft copolymers derived from commercial polymers offer an effective approach for incorporating specific properties into a material while retaining desirable properties of the parent polymer.<sup>1,2</sup> Compared to the parent polymer, graft copolymers often exhibit improvements such as enhanced compatibility with other polymers, adhesion to metallic and inorganic substrates, and dye retention.<sup>3</sup> In particular, the grafting of hydrophilic species onto hydrophobic polymers is of great utility. Amphiphilic graft copolymers so prepared often display enhanced surface properties, such as improved resistance to the adsorption of oils and proteins, biocompatibility, and reduced static charge buildup.

The synthesis of graft copolymers based on commercial polymers is most commonly accomplished free-radically. Free-radicals are produced on the parent polymer chains by exposure to ionizing radiation, and/or a free-radical initiator.<sup>3,4</sup> Alternatively, peroxide groups are introduced on the parent polymer by ozone treatment.<sup>5–9</sup> The resulting reactive sites serve as initiation sites for the free-radical polymerization of the comonomer. A significant disadvantage of these free-radical techniques is that homopolymerization of the comonomer always occurs to some extent, resulting in a product which is a mixture of graft copolymer and homopolymer. Moreover, backbone degradation and gel formation can occur as a result of uncontrolled free-radical production, often limiting the attainable grafting density.<sup>10</sup>

Because of its commercial importance, methods to prepare graft copolymers from PVDF have received some attention.<sup>5,9,11,12</sup> For example, using ozone-pre-treated PVDF, Liu et al.<sup>9</sup> prepared amphiphilic graft copolymers incorporating poly(oxyethylene methacrylate), a hydrophilic macromonomer. Under the grafting conditions used in that study, a limiting grafting density

of ~23 wt % comonomer was obtained. Preliminary experiments were performed on membranes prepared from these copolymers to assess their use as electrolytic membranes for lithium-ion batteries.

Atom transfer radical polymerization (ATRP) has recently been used to prepare graft copolymers from polymeric *macroinitiators*, polymer chains with regularly spaced, pendant chemical groups containing radically transferable halogen atoms.<sup>10,13,14</sup> The halogen atoms serve as initiation sites for the polymerization of side chains by ATRP. Thus, Matyjaszewski et al.<sup>13</sup> polymerized 2-(2-bromopropionyloxy)ethyl acrylate free-radically to obtain a macroinitiator with a pendant bromine atom on every repeat unit. The pendant bromine atoms were then used as initiation points for the ATRP of styrene and butyl acrylate side chains. Similarly, styrene and various methyl (meth)acrylate side chains have been grafted onto a poly[(vinyl chloride)-*co*-(vinyl chloroacetate)] macroinitiator, using the chloroacetate groups as initiation sites for ATRP of the monomers.<sup>14</sup> In these studies, no evidence of homopolymerization was observed, and the achievable grafting density was high due to the controlled nature of ATRP. A number of high-volume commercial polymers, including PVC, PVDF, and chlorinated polyolefins, comprise repeat units with secondary halogen atoms pendant. In principle, these polymers might be utilized as ATRP macroinitiators for the preparation of functionalized derivatives. However, it has been reported<sup>14</sup> that the secondary chlorine atoms of PVC are too strongly bonded to serve as ATRP initiation sites.

ATRP has also been used by a number of groups to polymerize hydrophilic monomers, including poly(oxyethylene) methacrylate macromonomers.<sup>15–17</sup> This paper demonstrates the direct preparation of amphiphilic graft copolymers having PVDF backbones by ATRP of hydrophilic side chains initiated at the secondary halogenated sites of PVDF. ATRP of a polyoxyethylene methacrylate (POEM) macromonomer incorporating roughly nine ethylene oxide (EO) units is used to prepare an amphiphilic graft copolymer, PVDF-*g*-

\* To whom correspondence should be addressed.

<sup>†</sup> Current address: 3M Center, Building 208-01-01, St. Paul, MN 55144-1000.

POEM. The grafting of *tert*-butyl methacrylate onto PVDF by ATRP is also used to prepare a polymer precursor which is subsequently hydrolyzed to obtain an amphiphilic, PVDF-based copolymer having poly(methacrylic acid) side chains, PVDF-*g*-PMAA.

These amphiphilic fluoropolymers have potential utility in the preparation of PVDF filtration membranes with engineered surface properties. Our previous studies<sup>18–21</sup> have shown that hydrophilic, protein-resistant surfaces can be generated on PVDF immersion precipitation membranes by adding to the casting solution small quantities ( $\leq 10\%$ ) of comb additive polymers, P(MMA-*r*-POEM), having poly(methyl methacrylate) (PMMA) backbones and PEO side chains. Surface segregation of the amphiphilic comb polymer during aqueous coagulation of the casting solution provides a protein-resistant, PEO-rich surface layer with no post-coagulation processing steps. Herein, we show that surface segregation of PVDF-*g*-POEM in PVDF membranes can be similarly accomplished during the standard immersion precipitation process, resulting in enhanced resistance to biofouling. Moreover, membranes containing as little as 5 wt % PVDF-*g*-POEM are spontaneously wettable by water. In a separate publication,<sup>22</sup> it is shown that PVDF membranes having pH-responsive separation characteristics can be prepared in a single step by the surface segregation of as little as 10% PVDF-*g*-PMAA to provide a brushlike layer of PMAA chains at the membrane surface.

## Experimental Section

**Materials.** PVDF<sub>250K</sub> ( $\bar{M}_n$  ca. 107 000 g/mol;  $\bar{M}_w$  ca. 250 000 g/mol); PVDF<sub>534K</sub> ( $\bar{M}_w$  ca. 534 000 g/mol); *tert*-butyl methacrylate (tBMA); poly(ethylene glycol) methyl ether methacrylate, referred to herein as poly(oxyethylene methacrylate) (POEM,  $\bar{M}_n = 475$  g/mol); poly(methyl methacrylate) standard (PMMA); copper(I) chloride (CuCl); 4,4'-dimethyl-2,2'-dipyridyl (DMDP); *p*-toluenesulfonic acid monohydrate (TSA); 1-methyl-2-pyrrolidinone (NMP, reagent grade); and toluene (anhydrous) were purchased from Aldrich Chemical Co. (Milwaukee, WI). Hexane, petroleum ether, ethanol, methanol, *N,N*-dimethylacetamide (DMAc), *N,N*-dimethylformamide (DMF), tetrahydrofuran (THF), hydrochloric acid, deuterated DMF, and lithium nitrate were purchased from VWR. Glycerol was purchased from Mallinckrodt. Bovine serum albumin (BSA) and phosphate-buffered saline were purchased from Sigma. All solvents were reagent grade, and all reagents were used as received. Deionized water (dW) was prepared using a Millipore (Bedford, MA) Milli-Q filtration system and had a resistivity of 18 M $\Omega$  cm.

**Synthesis of Graft Copolymers. PVDF-*g*-POEM.** PVDF<sub>250K</sub> (5 g) was dissolved in NMP (40 mL) in a conical flask at 50 °C. The solution was cooled to room temperature, after which POEM (50 mL), CuCl (0.04 g), and DMDP (0.23 g) were added and the flask was sealed with a rubber septum. Argon gas was bubbled through the reaction mixture for 15 min while stirring. The reaction vessel was then placed into an oil bath preheated to 90 °C, and the reaction was allowed to proceed for 19 h. The graft copolymer was precipitated into a mixture of 1 part methanol, 1–2 parts petroleum ether, and a small amount of HCl and recovered by filtration. The polymer was purified by thrice redissolving in NMP and reprecipitating in methanol/petroleum ether. Finally, the polymer was dried under vacuum overnight at room temperature; a conversion of 20% was obtained.

**PVDF-*g*-PMAA.** The preparation of PVDF-*g*-PMAA was a two-step synthesis. In the first step, poly(*tert*-butyl methacrylate) (PtBMA) side chains were graft copolymerized onto PVDF using ATRP. In the second step, the PtBMA side chains were hydrolyzed to yield PMAA. It is well-known<sup>23–26</sup> that PtBMA can be selectively and quantitatively hydrolyzed to PMAA in the presence of TSA.

PVDF<sub>250K</sub> (5 g), tBMA (50 mL), CuCl (0.04 g), and DMDP (0.23 g) were co-dissolved in NMP (40 mL) in a conical flask, as described above. The reaction vessel was similarly purged with argon gas, after which the reaction was performed at 90 °C for 20 h. The graft copolymer PVDF-*g*-PtBMA was precipitated into a 1:1 water:ethanol mixture, then purified by thrice redissolving in NMP and reprecipitating in 1:1 water:ethanol. The product was recovered by filtration and dried in a vacuum oven overnight at room temperature; a conversion of 42% was achieved.

Hydrolysis of PVDF-*g*-PtBMA (5.52 g) was performed in anhydrous toluene (300 mL). Pieces  $\sim 2$  mm in size were immersed in toluene, causing the polymer to swell visibly but not dissolve. TSA (31 g) was added to the reaction vessel, after which the reactor was immediately sealed with a rubber septum and the TSA was dissolved by vigorous stirring. Argon gas was bubbled through the reaction mixture for 15 min, after which the reactor was placed in an oil bath preheated to 85 °C. After 7 h, the heterogeneous reaction mixture was poured into excess methanol (a good solvent for TSA). The graft polymer PVDF-*g*-PMAA was recovered by filtration, redissolved in DMF, precipitated in a mixture containing 4 parts hexane and 1 part ethanol, and again recovered by filtration. For further purification, the polymer was stirred overnight in a large volume of THF (in which it swelled but did not dissolve), washed again in hexane/ethanol, and dried in a vacuum oven overnight at room temperature.

**Characterization of Graft Copolymers.** Gel permeation chromatography (GPC) of PVDF<sub>250K</sub>, PVDF-*g*-POEM, and PVDF-*g*-PMAA was conducted at 30 °C in DMF containing 1% lithium nitrate at a flow rate of 1 mL/min, using a Waters 510 HPLC pump, Waters Styragel columns, and a Waters 410 differential refractometer (Millipore Corp., Bedford, MA). <sup>1</sup>H NMR was performed on PVDF<sub>250K</sub> and its graft copolymers in deuterated DMF, using a Bruker DPX 400 spectrometer. Elemental analysis of PVDF<sub>250K</sub> and PVDF-*g*-POEM was performed by Quantitative Technologies Inc. (Whitehouse, NJ). Differential scanning calorimetry (DSC) was performed on PVDF<sub>250K</sub> and its derivatives using a Perkin-Elmer (Norwalk, CT) Pyris 1 calorimeter. To achieve a near-equilibrium structure prior to DSC analysis, the samples were preconditioned in the calorimeter by holding at 210 °C for 15 min, cooling to 130 °C at 10 °C/min, holding at 130 °C for 15 min, and cooling to 50 °C at 10 °C/min. DSC thermograms were then obtained while heating from 50 to 230 °C at 10 °C/min.

The morphology of PVDF-*g*-PMAA in the neat state was characterized using transmission electron microscopy (TEM). Thin film specimens for TEM were prepared via solvent casting at room temperature. A  $\sim 1$   $\mu$ L droplet of 0.01 wt % PVDF-*g*-PMAA solution in DMF was first placed on a 400-mesh copper TEM grid (Ted Pella, Inc.) and then dried for several days inside an isolated DMF atmosphere, then for a few hours under air, and finally for an hour under vacuum. This procedure resulted in the formation of a copolymer film approximately 50–100 nm thick, freely extended across the metal grid. TEM measurements were performed in the bright field mode on a JEOL 100CX microscope operated at 200 kV. Images were obtained for the unstained sample at a slight underfocus through the mechanism known as phase contrast.<sup>27</sup>

TEM was performed on PVDF-*g*-POEM using a JEOL 200CX microscope operated in the bright field mode at an accelerating voltage of 100 kV. Prior to TEM characterization, a bulk polymer sample was equilibrated in a vacuum oven at 200 °C for 12 h. It was then cryomicrotomed into 50 nm thick sections at  $-55$  °C using a RMC (Tucson, AZ) MT-XL ultramicrotome. The sections were mounted on copper grids and stained with ruthenium tetroxide for 20 min at room temperature.

**Sample Preparation. Evaporation Cast Films.** PVDF-*g*-POEM films for X-ray photoelectron spectroscopy (XPS) studies were prepared on glass coverslips by evaporation casting. The graft copolymer was dissolved in DMAc at a concentration of 0.05 g/mL. The resulting solution was then cast onto the glass substrates, and the DMAc was allowed to evaporate slowly at room temperature over a period of  $\sim 48$  h.



**Table 1. Compositions of Membrane Casting Solutions**

	g/100 g of casting solution		
	I	II	III
PVDF	18.0	18.0	18.0
PVDF- <i>g</i> -POEM		0.95	2.0
glycerol	3.3	1.0	1.0
DMAc	78.7	80.1	79.0

Finally, the polymer films were held under vacuum at room temperature for 96 h to remove residual solvent. Because of the low volatility of DMAc and the consequently long evaporation times, surface compositions of the resulting films were expected to be near equilibrium.

**Membranes.** Membranes were prepared from casting solutions containing PVDF<sub>534K</sub>, PVDF-*g*-POEM, glycerol, and DMAc according to the compositions listed in Table 1. Each casting solution was passed through a 10  $\mu$ m, binder-free, glass fiber filter (Type APFD Prefilter, Millipore) by means of a stainless steel filter holder (Millipore) pressurized with nitrogen gas, then heated to 50–70 °C for at least 4 h until no gas bubbles were visible in the solution. Each solution was cast onto a first surface optical mirror (Edmund Scientific Co., Barrington, NJ) under a casting bar having an 8-mil (~200- $\mu$ m) gate size. The mirror was then immersed immediately into a bath of dW at 90 °C. (The elevated coagulation bath temperature enhances surface segregation of the comb additive, as shown previously.<sup>18,20,21</sup>) After coagulation, each membrane was removed from the bath after complete separation from the mirror and immersed overnight in a second dW bath at 20 °C, followed by air-drying.

**Sample Characterization. X-ray Photoelectron Spectroscopy.** XPS was performed on membranes and films to determine their near-surface compositions. XPS was conducted on a Surface Science Instruments SSX-100 spectrometer (Mountain View, CA) using monochromatic Al K $\alpha$  X-rays ( $h\nu$  = 1486.7 eV) with an electron takeoff angle of 45° relative to the sample plane. Survey spectra were run in the binding energy range 0–1000 eV, followed by high-resolution spectra of the C 1s region. Peak fitting of the C 1s region was conducted with a linearly subtracted background and with each component of the C 1s envelope described by a Gaussian–Lorentzian sum function, as detailed in previous publications.<sup>18,21</sup>

**Scanning Electron Microscopy.** Field emission scanning electron microscopy (FESEM) was used for the characterization of membrane separation surface and cross-sectional morphologies. Fracture surfaces for cross-sectional imaging were prepared by cracking membranes under liquid nitrogen. Samples were sputter-coated with ~50 Å of gold–palladium using a Pelco SC-7 auto sputter coater. Coated samples were examined at an accelerating voltage of 1 kV using a JEOL 6320 FESEM.

**Contact Angle Measurements.** Water contact angle measurements were performed on membranes using an Advanced Surface Technologies, Inc., VCA2000 video contact angle system. Each sample was raised toward a 1- $\mu$ L droplet of dW suspended from the tip of the syringe until the droplet was transferred to the sample surface. Advancing contact angles were then measured after adding dW to the droplet in 1- $\mu$ L increments until its edges were observed to advance over the surface.

**Static Protein Adsorption Measurements.** To investigate the protein adsorption resistance of membranes containing PVDF-*g*-POEM, membranes were immersed in a solution containing bovine serum albumin. Membranes were first hydrated by immersion in methanol followed by immersion in dW. Membranes were subsequently washed with phosphate-buffered saline (0.01 M PBS pH 7.4) for 1 h, then incubated in PBS containing 10.0 g/L of BSA for 24 h at room temperature, and washed for 5 min in three changes of PBS followed by three changes of dW. Finally, samples were dried in a vacuum oven at room temperature. Surface coverage of BSA was quantified using XPS, by detection of nitrogen occurring in BSA. Survey spectra were run in the binding energy range

**Table 2. Properties of Base Polymer and Graft Copolymers**

polymer	composition (wt % comonomer)	GPC molar mass (g/mol) <sup>a</sup>		actual molar mass (est, g/mol)M <sub>n</sub>
		M <sub>n</sub>	M <sub>w</sub> /M <sub>n</sub>	
PVDF <sub>250K</sub>		580 100	2.10	107 000 <sup>b</sup>
PVDF- <i>g</i> -POEM	71	2 159 300	1.38	323 200 <sup>c</sup>
PVDF- <i>g</i> -PMAA	51	2 709 100	1.11	211 300 <sup>c</sup>

<sup>a</sup> From GPC, based on PMMA standards. <sup>b</sup> From the manufacturer. <sup>c</sup> Estimated based on composition from <sup>1</sup>H NMR using eq 4.

0–1000 eV, and the near-surface atomic compositions were determined using numerically integrated peak areas and applying standard sensitivity coefficients.

## Results and Discussion

**Graft Copolymer Characterization. Composition. PVDF-*g*-POEM.** The <sup>1</sup>H NMR spectra for PVDF and PVDF-*g*-POEM appear in Figure 1. The PVDF spectrum exhibits two well-known peaks<sup>28</sup> due to head-to-tail (ht) and head-to-head (hh) bonding arrangements. Grafting of POEM to PVDF resulted in the appearance of peaks in the region 3.2–4.3 ppm due to the O–CH<sub>x</sub> bonding environments in the methacrylate<sup>28</sup> and PEO<sup>29</sup> moieties of POEM. The solvent peaks **s**<sub>2</sub> and **s**<sub>3</sub> were subtracted from the spectra using their known intensities relative to solvent peak **s**<sub>1</sub> obtained by analysis of pure deuterated DMF. The mole fraction of POEM in the copolymer was then calculated as 0.248 based on the intensities of resonances **a**(ht), **a**(hh), **c**, **d**, and **e**. The composition so calculated is shown in Table 2, converted to a mass basis.

**PVDF-*g*-PMAA.** <sup>1</sup>H NMR spectra for PVDF, PVDF-*g*-PtBMA, and PVDF-*g*-PMAA appear in Figure 2. Grafting of tBMA to PVDF resulted in the appearance of a peak at 1.5 ppm in part b due to the *tert*-butyl protons.<sup>23–26,30</sup> Despite the heterogeneous nature of the hydrolysis reaction, hydrolysis of the PtBMA side chains to PMAA was quantitative, as indicated by the complete disappearance of the *tert*-butyl peak in part c. The spectrum for PVDF-*g*-PMAA also contains a resonance at 12.6 ppm due to the carboxylic acid proton.<sup>26</sup>

For spectra b and c, the solvent resonance **s**<sub>3</sub> was subtracted based on its known intensity relative to solvent peak **s**<sub>1</sub> established by NMR analysis of pure deuterated DMF. The mole fraction of tBMA in PVDF-*g*-PtBMA was then calculated from Figure 2b based on the intensities of resonances **a**(ht), **a**(hh), and **b**. Similarly, the mole fraction of MAA in PVDF-*g*-PMAA was calculated from Figure 2c based on resonances **a**(ht), **a**(hh), and **e**. The calculated mole fractions of PtBMA and PMAA were 0.403 and 0.438, respectively. The close agreement between the two values provides strong evidence that the hydrolysis reaction was selective and quantitative, and that the MAA units of the hydrolyzed copolymer were protonated. The composition shown in Table 2 is based on an average of the compositions calculated using Figure 2, parts b and c.

**Molecular Weight.** GPC traces for PVDF<sub>250K</sub>, PVDF-*g*-POEM, and PVDF-*g*-PMAA are shown in Figure 3. The PMMA standard molecular weight and polydispersity of each polymer, obtained directly from the GPC trace, appear in Table 2. The grafting of both POEM and PMAA to PVDF resulted in distributions shifted up significantly in molecular weight relative to the PVDF homopolymer. The molecular weight distribution (MWD) of PVDF-*g*-POEM (Figure 3b) was multimodal.

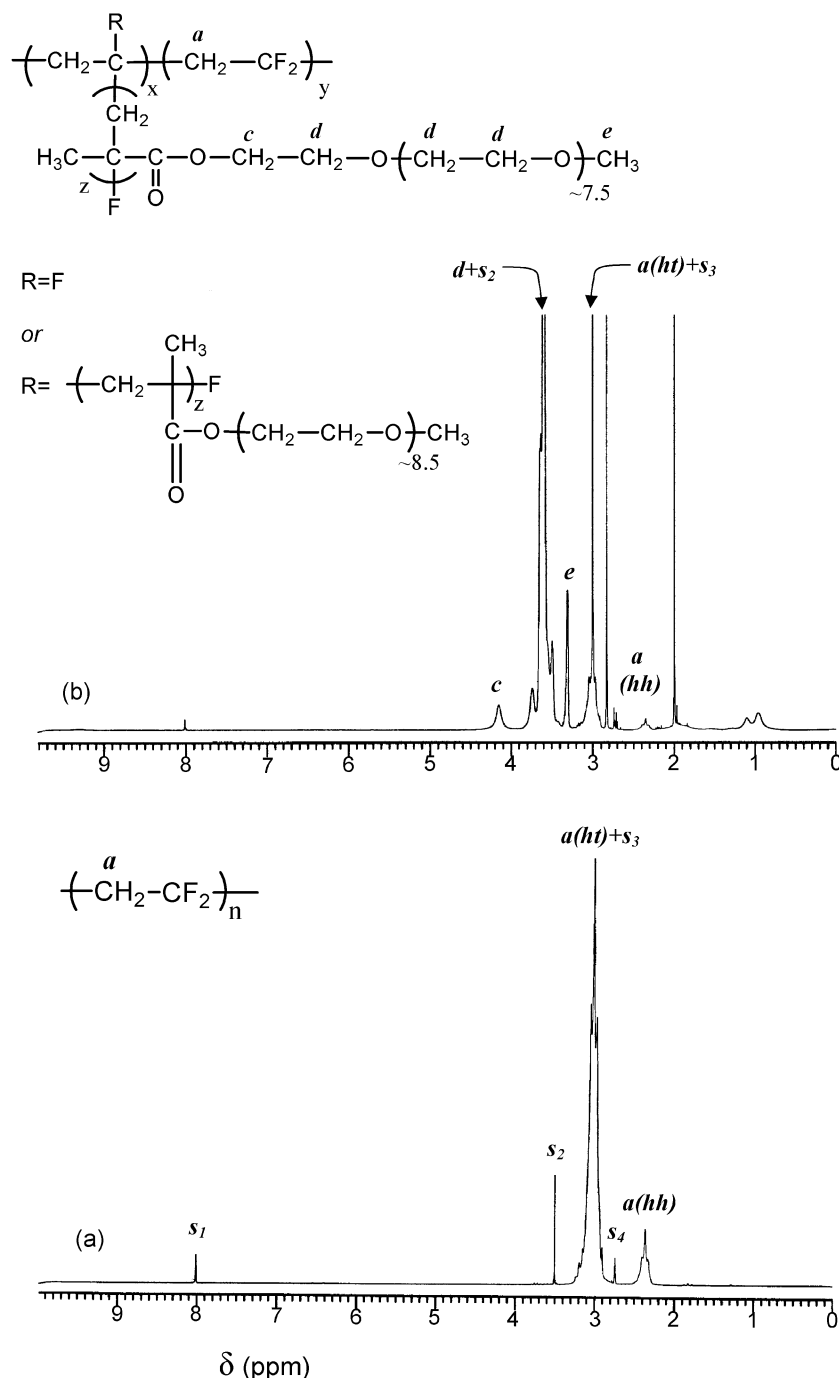


**Figure 1.** 400 MHz  $^1\text{H}$  NMR spectra for (a) PVDF<sub>250K</sub> and (b) PVDF-*g*-POEM. Resonances labeled  $s_n$  are solvent peaks due to deuterated DMF. One or both of the fluorine atoms on each repeat unit may act as an initiation site for monomer addition (b, inset, chemical structure).

The GPC trace was virtually unchanged (Figure 3c) after a 48-h extraction in a large volume of dW, a good solvent for poly(POEM), indicating that its multimodality was not due to homopolymerization of POEM. Instead, this distribution was likely a result of radical-radical coupling of chains during polymerization, which has been observed previously in graft copolymerizations by ATRP, and which can result in multimodal MWDs.<sup>13</sup> The MWD for PVDF-*g*-PMAA (Figure 3d) was monomodal, providing no evidence of homopolymer contamination or coupling reactions.

Because of the difference in chain flexibility between PVDF and PMMA and differences between the hydrodynamic radii of linear and branched polymers of equal molecular weight, the PMMA standard molecular weights

are not accurate estimates of the true molecular weights of the graft copolymers. More accurate estimates of their number-average molecular weights were obtained from NMR using the relationship,

$$\bar{M}_{n,\text{graft}} = \bar{M}_{n,\text{PVDF}} \left( 1 + x \frac{M_0^{\text{comonomer}}}{M_0^{\text{PVDF}}} \right) \quad (1)$$

where  $\bar{M}_{n,\text{PVDF}}$  is the number-average molecular weight of the parent PVDF obtained from the manufacturer,  $x$  is the molar ratio of comonomer units to PVDF repeat units in the copolymer as measured by NMR, and  $M_0^{\text{PVDF}}$  and  $M_0^{\text{comonomer}}$  are the repeat unit molar masses of PVDF and the comonomer, respectively. The graft

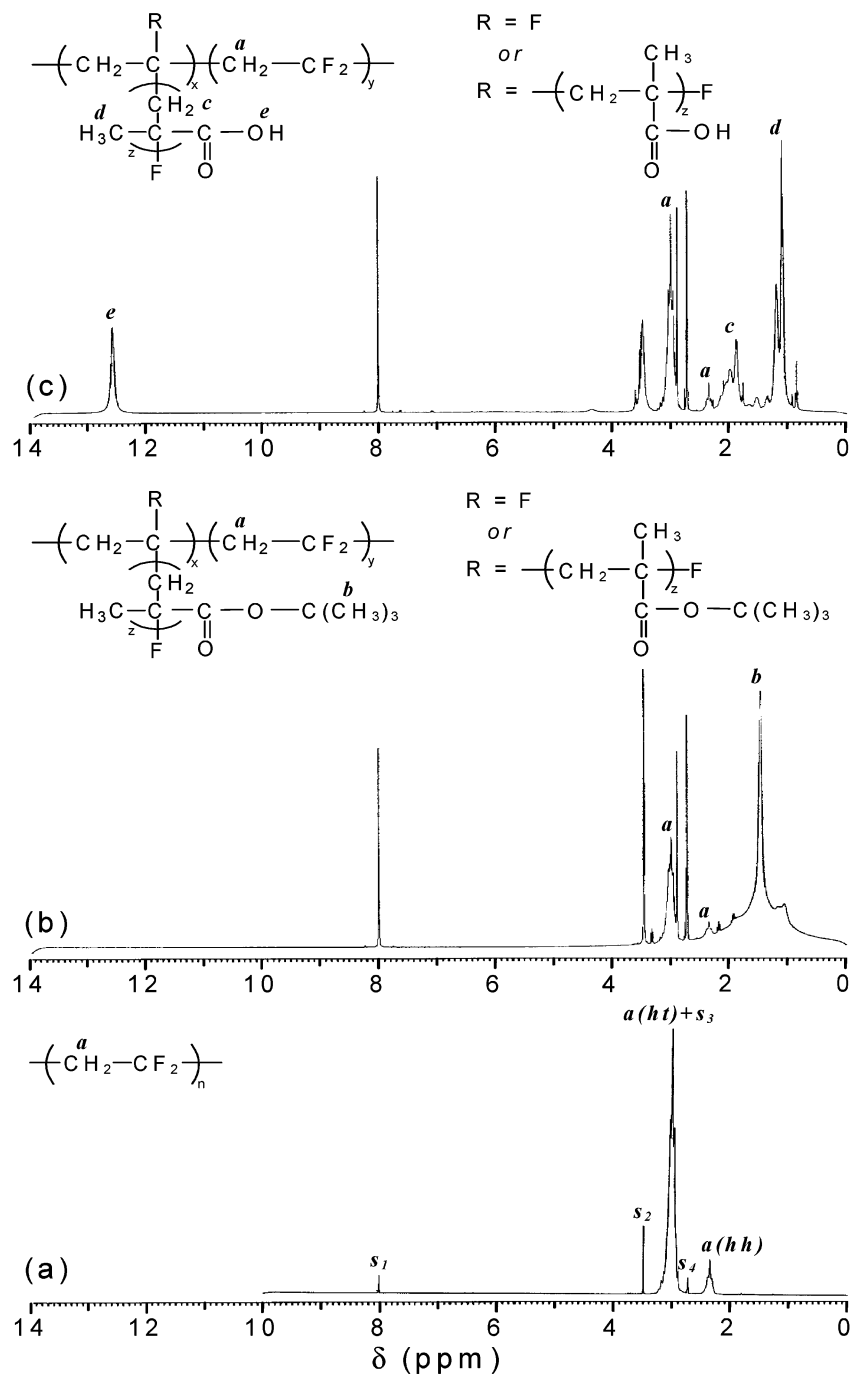


**Figure 2.** 400 MHz  $^1\text{H}$  NMR spectra for (a) PVDF<sub>250K</sub>, (b) PVDF-*g*-PtBMA, and (c) PVDF-*g*-PMAA. Resonances  $s_n$  are solvent peaks due to deuterated DMF. Quantitative hydrolysis of PtBMA to PMAA is confirmed by the disappearance in part c of the *tert*-butyl peak **b** and the appearance of the acid proton peak **e**.

copolymer molecular weights so calculated appear in Table 2.

The graft copolymer MWDs obtained from GPC appear narrow relative to that of the PVDF<sub>250K</sub> base polymer. This is not expected, as the MWD of a graft copolymer should not be appreciably lower than the base polymer.<sup>13</sup> The apparently narrow MWDs of the graft copolymers are most likely a result of preferential extraction of low molecular weight product during the repeated precipitations and extractions used to purify the products.

**Crystallinity.** DSC thermograms for PVDF<sub>250K</sub>, PVDF-*g*-POEM, and PVDF-*g*-PMAA appear in Figure 4. For each polymer, the weight percent crystallinity,

with respect to the PVDF content of the polymer, was computed as

$$W_c = \frac{M_0^{\text{PVDF}} \Delta H_m}{W_{\text{PVDF}} \Delta H_f^*} \quad (2)$$

where  $W_{\text{PVDF}}$  is the weight fraction of PVDF in the polymer from NMR,  $\Delta H_m$  is the heat of melting observed by DSC [J/g], and  $\Delta H_f^*$  is the heat of fusion of PVDF (6700 J/mol<sup>31</sup>). Both PVDF-*g*-POEM and PVDF-*g*-PMAA retained substantial crystalline content. However, the two graft copolymers differed significantly in their melting point depressions relative to the PVDF parent



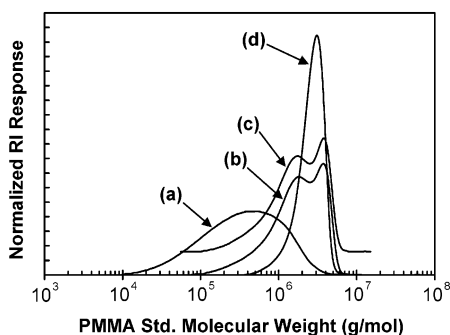


**Figure 3.** GPC traces for (a) PVDF<sub>250K</sub>, (b, c) PVDF-*g*-POEM, and (d) PVDF-*g*-PMAA. Trace b is PVDF-*g*-POEM following purification as described in the text, while trace c, offset for clarity, is PVDF-*g*-POEM after an additional 48-h extraction in a large volume of water. The molecular weight scale was calibrated using PMMA standards.

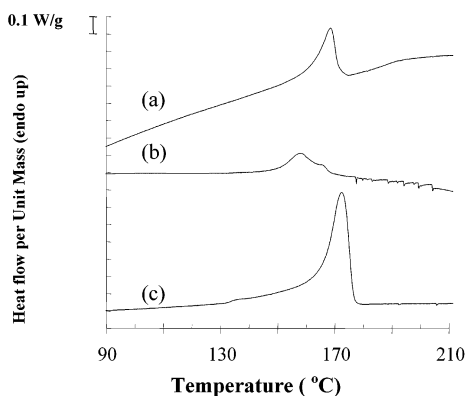


**Figure 4.** DSC thermograms upon heating for (a) PVDF<sub>250K</sub>,  $T_m = 172$  °C,  $\Delta H_m = 50.6$  J/g, 48% crystallinity; (b) PVDF-*g*-POEM,  $T_m = 158$  °C,  $\Delta H_m = 10.6$  J/g, 10% crystallinity (31% with respect to PVDF); and (c) PVDF-*g*-PMAA,  $T_m = 168$  °C,  $\Delta H_m = 15.6$  J/g, 15% crystallinity (29% with respect to PVDF).

polymer. While PVDF-*g*-POEM exhibited substantial melting point depression, PVDF-*g*-PMAA exhibited only slight melting point depression.

**Morphology and Architecture.** The side chain length of graft copolymers prepared by direct ATRP onto PVDF is unpredictable a priori. The abundance of potential side chain initiation sites (two per PVDF repeat unit) competes with the low reactivity of those sites compared with that of the propagating side chain ends, the terminal carbon atoms of which are adjacent to radical-stabilizing carbonyl groups.<sup>14,32</sup> The absence of appreciable melting point depression in the DSC trace of PVDF-*g*-PMAA suggests that PMAA grafting points along the PVDF backbone were infrequent. In contrast, the significant melting point depression observed for PVDF-*g*-POEM suggests more frequent grafting points along the PVDF backbone.

This is further supported by our TEM studies. A TEM image of the microphase-segregated morphology formed at room temperature in the solvent-cast PVDF-*g*-PMAA film is shown in Figure 5. The morphology appears highly defected and lacking in long-range order, similar to morphologies observed in other recently synthesized comb polymers having incompatible backbone/side chain pairs.<sup>33–35</sup> The expected difference in electron density between the two chemistries facilitates image interpretation, with PVDF domains appearing as darker regions in the figure. The mean separation between the darker regions is therefore taken as a characteristic measure

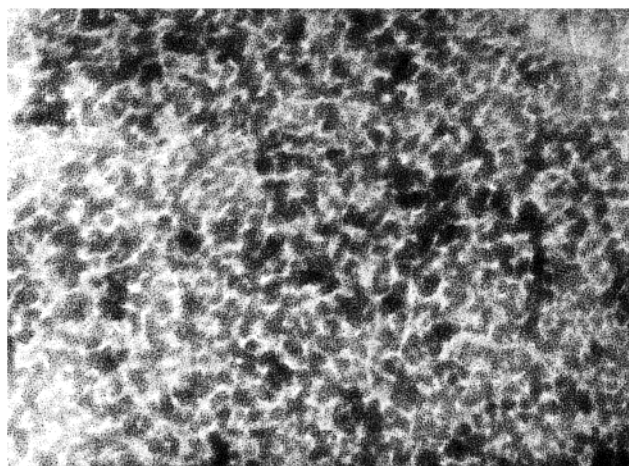


**Figure 5.** TEM micrograph of PVDF-*g*-PMAA. PVDF microdomains appear as darker regions in the image.

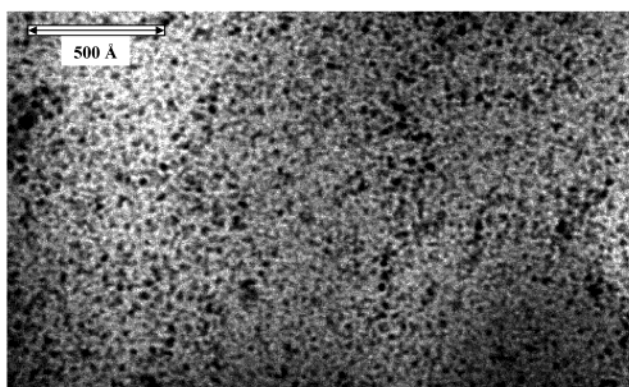


**Figure 6.** TEM micrograph of PVDF-*g*-POEM stained with ruthenium tetroxide. The stained POEM microdomains appear as darker regions in the image.

of the PMAA domain size, estimated to be approximately 200 Å. Assuming that this cross-sectional dimension is approximately equal to twice the end-to-end distance of the PMAA arm in a random-walk configuration,<sup>36,37</sup> we estimate a molar mass of  $\sim 24\,000$  g/mol per side chain, or  $\sim 270$  MAA segments, using a characteristic ratio of  $\sim 7.5$  for PMAA and a value for the carbon-carbon bond length of 1.54 Å (both estimated from published data for similar polymers<sup>38</sup>). The estimate of 270 segments represents an upper limit, as components of a block copolymer in the microphase-separated state are typically stretched relative to their random coil dimensions perpendicular to the block-block interface. Using this estimate, the measured copolymer composition and PVDF molecular weight, we calculate the approximate number of arms per chain to be about 4. Indeed, Figure 3 implies an architecture in which long PMAA side chains are grafted sparsely along the PVDF backbone. Mass transport and force microscopy measurements conducted on membranes having surfaces rich in PVDF-*g*-PMAA, presented elsewhere,<sup>21,22</sup> support these structural measurements.

Figure 6 is a TEM micrograph of PVDF-*g*-POEM stained with ruthenium tetroxide, which selectively stains the ether oxygen moieties in PEO, and which has been shown not to stain PVDF.<sup>39</sup> The micrograph shows an apparently microphase-segregated structure with stained POEM domains appearing dark. The domain size is roughly 20 Å, consistent with a “poly(POEM)” side chain length of only 1 POEM unit. Elemental

Table 3. Elemental Analysis Results

polymer	anal., wt %			
	C	H	F	Cl
PVDF <sub>250K</sub> (calcd)	38.71	3.23	58.06	
PVDF <sub>250K</sub>	37.37 ± 0.05	2.69 ± 0.13	57.85 ± 0.20	
PVDF- <i>g</i> -POEM	49.94 ± 0.06	7.64 ± 0.10	16.04 ± 0.17	0.23 ± 0.01

analysis (Table 3) of PVDF-*g*-POEM indicated a POEM content of 72.6 wt % (26.3 mol %) based on F content, and assuming an average side chain length of one POEM segment. This value is in good agreement with the <sup>1</sup>H NMR value of 71 wt % POEM. The combined results from elemental analysis and TEM suggest the grafting of 1 POEM unit for every 3 VDF repeat units.

**Initiation of ATRP by Secondary Fluorine.** The combined GPC, TEM, NMR, and elemental analysis results indicate unambiguously that POEM and PtBMA are grafted to the PVDF base polymer, apparently by ATRP initiation at the secondary fluorinated site. To our knowledge, ATRP initiation by secondary fluorine has not been previously reported. Moreover, such initiation has not been observed in previous studies<sup>40–43</sup> involving macroinitiators containing PVDF. In these studies, various synthetic routes were used to produce PVDF polymers or oligomers terminated with iodine,<sup>40</sup> bromine,<sup>41</sup> trichloromethyl groups,<sup>42</sup> or benzyl chloride.<sup>43</sup> ATRP was then used to initiate polymerization of various (meth)acrylate and styrene monomers at the macroinitiator end sites, yielding di- and triblock copolymers. Because of the expected high reactivity with respect to ATRP radical generation of the iodinated, brominated, and chlorinated end sites used in these studies relative to secondary fluorine, it is not surprising that polymerization appeared to initiate exclusively (or nearly exclusively) at these more reactive sites. Moreover, the characterization techniques used in these studies (GPC, <sup>1</sup>H NMR, and DSC) would not be capable of detecting low concentrations of fluorine-initiated side chains. (Consider PVDF-*g*-PMAA synthesized herein, the above TEM results for which indicate initiation at only ~0.1% of the available secondary fluorinated sites per chain.)

Once growth of a side chain is initiated, halogen exchange between fluorine and chlorine in the CuCl catalyst is considered unlikely due to stronger C–F binding energy<sup>44</sup> (486 vs 339 kJ/mol for C–Cl). Furthermore, the strong C–F bond delays the rate of radical initiation compared to the rate of propagation, limiting the “living” nature of the reaction. Probably owing to the low initiation efficiency of secondary fluorine, the graft copolymerizations by ATRP performed herein yielded low monomer conversions (20% conversion after 19 h for PVDF-*g*-POEM and 42% conversion after 20 h for PVDF-*g*-PtBMA). Despite these shortcomings, the direct graft copolymerization of PVDF by ATRP is potentially a very useful technique, enabling the economical, single-step production of functionalized derivatives having comonomer concentrations often difficult to achieve by other grafting methods.

A hypothesis for the apparent kinetic difference between the PVDF/POEM and PVDF/tBMA systems is that, in the former system, steric hindrance of the terminal halogenated carbon atom of the growing side chain by the pendant PEO reduces the reactivity of that site in propagation, relative to the corresponding site in the PVDF/tBMA system. Moreover, in these studies the mole ratio of initiator to monomer was lower in the

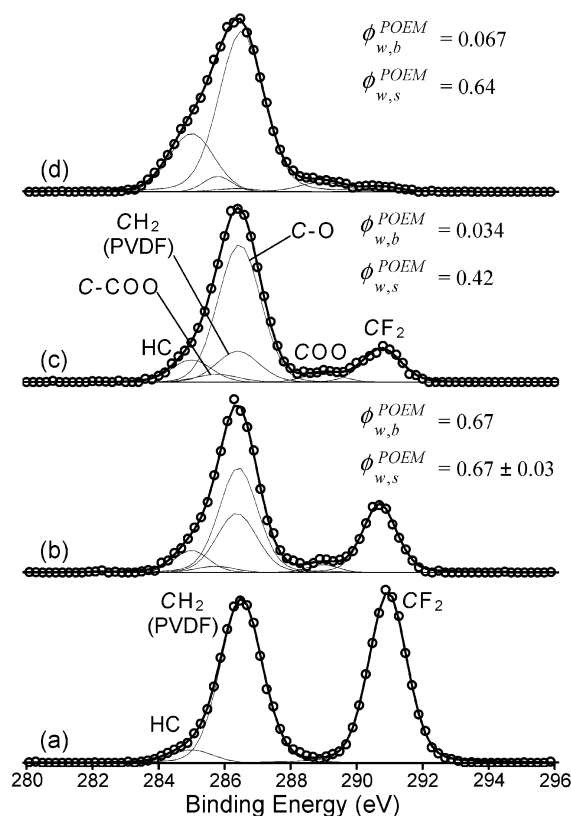


**Figure 7.** Fitted C 1s envelopes for (a) a pure PVDF membrane, (b) an evaporation cast film of PVDF-*g*-POEM, and membranes containing (c) 5 wt % and (d) 10 wt % PVDF-*g*-POEM. For parts b–d, the computed bulk and surface compositions are noted in terms of weight fraction of POEM. For part b, the surface composition is an average from two samples.

case of PVDF/tBMA, which would also be expected to yield relatively longer side chains.

Further work is needed to elucidate ATRP initiation by secondary fluorine, such as the ATRP of methacrylate monomers using small-molecule initiators containing secondary fluorine. Measurement of the initiation efficiencies of such model initiators and the MWDs of the resulting homopolymers would provide needed clarity regarding secondary fluorine-initiated ATRP.

The remainder of this paper considers the utility of the graft copolymers produced herein as surface-modifying additives for PVDF membranes prepared by immersion precipitation.

**Membranes Containing PVDF-*g*-POEM. Near-Surface Composition.** The near-surface compositions of PVDF membranes containing 5–10 wt % PVDF-*g*-POEM, as well as an evaporation cast sample of pure PVDF-*g*-POEM, were determined by fitting the C 1s regions of their XPS spectra as shown in Figure 7.<sup>18,21</sup> For membranes, XPS analysis was conducted on the side of the membrane facing the water bath during the precipitation step of fabrication. In membrane separations, it is this side of the membrane that contacts the feed solution.



**Table 4. Membrane Wetting Properties**

membrane type	$\phi_{w,b}^{\text{POEM}}$	$\phi_{w,s}^{\text{POEM}}$	$\theta_{\text{adv, initial}}^a$ (deg)	wetting time <sup>b</sup> (s)
I	0	0	89.9 ± 4.1	nonwetting
II	0.034	0.42	60.4 ± 2.3	147 ± 83
III	0.067	0.64	53.5 ± 7.0	16 ± 10

<sup>a</sup> Initial advancing contact angle of a 1- $\mu$ L dW droplet placed on the membrane surface. <sup>b</sup> Time required for a 1- $\mu$ L dW droplet placed on the membrane surface to reach a contact angle of 0°.

From the fitted C 1s spectra, the near-surface mole fraction of POEM was calculated as

$$X_s^{\text{POEM}} = \frac{A_{\text{COO}}}{A_{\text{COO}} + A_{\text{CF}_2}} \quad (3)$$

where  $A_{\text{COO}}$  and  $A_{\text{CF}_2}$  are the areas of the fitted COO and CF<sub>2</sub> peaks, respectively. The near-surface POEM concentrations ( $\phi_{w,s}^{\text{POEM}}$ ), converted to weight fraction, are given in Figure 7, along with the bulk POEM weight fractions ( $\phi_{w,b}^{\text{POEM}}$ ). Clearly, significant surface segregation of the amphiphilic graft copolymer in PVDF occurs during the single-step fabrication of the membranes by immersion precipitation, due to the relatively low interfacial energy between the amphiphilic component and water.<sup>18,21</sup> Indeed, the membrane containing 10 wt % PVDF-*g*-POEM has a near-surface POEM concentration roughly identical to that of the pure graft copolymer.

The membrane surface chemistries achieved by surface segregation of PVDF-*g*-POEM may be compared to results obtained recently<sup>9</sup> on membranes cast from a pure graft copolymer which was structurally similar to PVDF-*g*-POEM, prepared using a conventional free-radical method following ozone pretreatment of PVDF. The macromonomer used in that study differed only in the length of its pendant PEO chain (~five EO units, rather than ~nine units herein). Membranes prepared by immersion precipitation of the conventionally prepared graft copolymer had a near-surface comonomer weight fraction of  $\phi_{w,s} = 0.50$  for a bulk comonomer weight fraction of  $\phi_{w,b} = 0.23$ , the limiting graft copolymer composition achieved under the grafting conditions used. Comparison of these values to those reported in Table 4 shows that, herein, greater surface expressions of POEM (>60 wt %) were achieved for blends containing much lower bulk concentrations of the comonomer (<7 wt %). This comparatively high surface enrichment is likely due to the higher POEM grafting density obtained by ATRP and to the elevated temperature of the coagulation bath.<sup>18,20,21</sup>

**Morphology.** FESEM micrographs of the separation surfaces and cross sections of membranes cast under identical conditions but having different bulk fractions of PVDF-*g*-POEM are shown in Figure 8. Addition of the graft copolymer results in substantial increases in separation surface porosity at relatively constant pore size, as well as more pronounced macrovoid formation

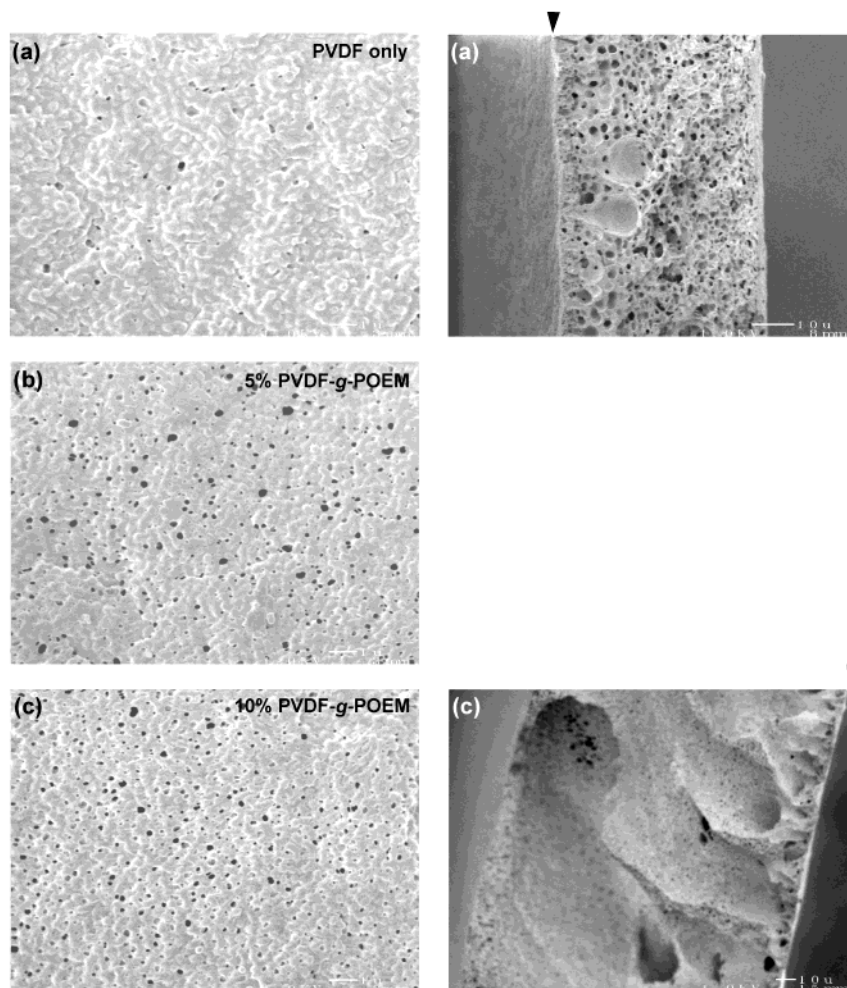


**Figure 8.** FESEM images of the separation surfaces (left) and cross sections (right) of (a) a pure PVDF membrane and membranes containing (b) 5 wt % and (c) 10 wt % PVDF-*g*-POEM. Arrows indicate the separation surface in cross-sectional images.



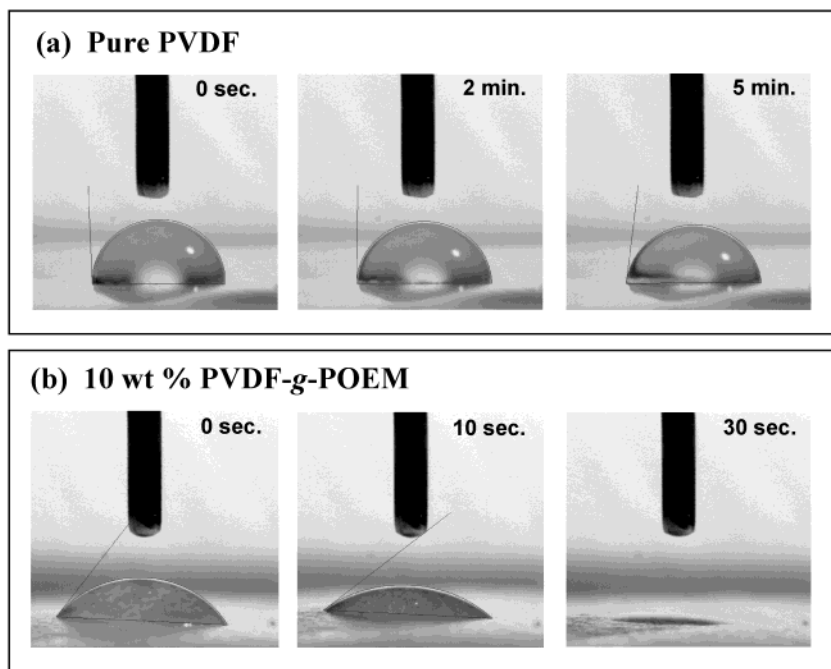


**Figure 9.** Images of 1- $\mu$ L water droplets at various times on (a) a pure PVDF membrane and (b) a membrane having a bulk composition of 10 wt % PVDF-*g*-POEM.

in the membrane substructure. Similar morphological changes are observed with the addition to PVDF membranes of PVDF-*g*-PMAA,<sup>22</sup> as well as methacrylic comb polymers having PEO side chains.<sup>18,20,21</sup> This enhancement of membrane porosity is highly advantageous in filtration applications, as it provides for substantially higher fluxes.<sup>20,21</sup>

**Wettability.** A droplet of water placed on a pure PVDF membrane assumes a high contact angle, which changes very little over time until the drop finally evaporates. For this reason, the hydration of PVDF membranes from the dry state generally requires prewetting, typically with a surfactant or an alcohol. In contrast, a water droplet placed on a membrane containing 5–10 wt % PVDF-*g*-POEM assumes a moderate initial contact angle ( $>50^\circ$ ) which decreases to zero over time, and the droplet ultimately wets through the membrane (see Figure 9). In this study, wettability was assessed based on the initial advancing contact angle of a 1  $\mu$ L water droplet placed on the membrane surface, as well as the time required for the contact angle of the droplet to reach  $0^\circ$ . These values are reported in Table 4. The delayed wetting behavior of membranes modified with PVDF-*g*-POEM indicates local surface reorganization to express POEM upon contact with water.

**Static Fouling Resistance.** The presence of POEM at the membrane surface results in significant resistance to protein adsorption. The near-surface nitrogen content of membranes exposed to a 10 g/L BSA solution for 24 h were obtained by integration of the following peaks in the XPS survey spectra: C 1s (285 eV), N 1s (399 eV), O 1s (531 eV), and F 1s (685 eV). Like PVDF-based membranes prepared from casting compositions containing other amphiphilic comb polymers,<sup>18–21</sup> membranes modified by surface segregation of PVDF-*g*-POEM show substantially enhanced resistance to BSA adsorption compared to pure PVDF membranes. Membranes with a bulk composition of 5 wt % PVDF-*g*-POEM (3.4 wt % POEM) adsorb BSA at a level less than 25% that of PVDF-only membranes, while incorporation

of 10 wt % PVDF-*g*-POEM yields a  $\sim 7$ -fold reduction in BSA adsorption.

## Conclusion

Graft copolymerization onto PVDF by ATRP initiation of methacrylic side chains at the secondary halogenated site has been demonstrated. This technique offers an effective and commercially relevant alternative to conventional free radical routes for the preparation of graft copolymers based on PVDF, as the grafting of large proportions (nearly 70 wt % in one demonstrated case) of the comonomer may be accomplished without any unusual care with respect to the purity of the reagents.

Using this method, PVDF-*g*-POEM has been synthesized by graft copolymerization of a methacrylate monomer having a short pendant PEO chain. The hydrophilic surface modification of PVDF filtration membranes using PVDF-*g*-POEM is highly effective, due to the opportunity afforded by the standard immersion precipitation process to effect surface segregation of the graft copolymer additive during membrane fabrication. Thus, a PVDF/5 wt % PVDF-*g*-POEM membrane, fabricated with no extra processing steps and having a bulk POEM concentration of only 3.4 wt %, exhibits a near-surface POEM concentration of 42 wt % as measured by XPS. This membrane adsorbs roughly four times less BSA than a pure PVDF membrane during a 24 h static protein adsorption experiment, and spontaneously wets when placed in contact with water. On the basis of these results, PVDF-*g*-POEM prepared using ATRP is an excellent candidate for the surface modification of PVDF filtration membranes to render them wettable and fouling-resistant.

A second amphiphilic graft copolymer, PVDF-*g*-poly(methacrylic acid), has been prepared using the direct ATRP grafting of hydrolyzable poly(*tert*-butyl methacrylate) side chains onto PVDF. The application of this polymer for the facile preparation of pH-responsive membranes is explored in a separate publication.<sup>22</sup> In that article, we show that incorporation of as little as

10 wt % PVDF-*g*-PMAA into a PVDF blend enables the *single-step* preparation of PVDF-based membranes having pH-responsive separation characteristics similar to membranes fabricated using process-intensive surface graft polymerization techniques.

**Acknowledgment.** Financial support for this work was provided by the U.S. Office of Naval Research under Awards N00014-99-1-0310 and N00014-02-1-0343. This work made use of MRSEC Shared Experimental Facilities supported by the National Science Foundation under Award DMR-98-08941.

#### Note Added After ASAP Posting

This article as released ASAP on 08/24/2002 without the Acknowledgment. The correct version was posted on 09/04/2002.

#### References and Notes

- (1) Battard, H. A. J.; Tregar, G. W. *Graft Copolymers*; Wiley-Interscience: New York, 1967.
- (2) Ceresa, R. J. *Block and Graft Copolymerization*; Wiley-Interscience: New York, 1973; Vol. I.
- (3) Xu, G. X.; Lin, S. G. *J. Macromol. Sci.—Rev. Macromol. Chem. Phys.* **1994**, C34, 555–606.
- (4) Mukherjee, A. K.; Gupta, B. D. *J. Macromol. Sci.—Chem.* **1983**, A19, 1069–1099.
- (5) Boutevin, B.; Robin, J. J.; Serdani, A. *Eur. Polym. J.* **1992**, 28, 1507.
- (6) Fargere, T.; Abdennadher, M.; Delmas, M.; Boutevin, B. *J. Polym. Sci., Part A: Polym. Chem.* **1994**, 32, 1337.
- (7) Kang, E. T.; Neoh, K. G.; Tan, K. L.; Loh, F. C. *Synth. Met.* **1997**, 84, 59.
- (8) Wang, T.; Kang, E. T.; Neoh, K. G.; Tan, K. L.; Liaw, D. J. *Langmuir* **1998**, 14, 921.
- (9) Liu, Y.; Lee, J. Y.; Kang, E. T.; Wang, P.; Tan, K. L. *React. Funct. Polym.* **2001**, 47, 201–213.
- (10) Wang, X.-S.; Luo, N.; Ying, S.-K. *Polymer* **1999**, 40, 4515–4520.
- (11) Mascia, L.; Hashim, K. *J. Appl. Polym. Sci.* **1997**, 66, 1911–1923.
- (12) Valenza, A.; Carianni, G. *Polym. Eng. Sci.* **1998**, 38, 452–460.
- (13) Beers, K. L.; Gaynor, S. G.; Matyjaszewski, K. *Macromolecules* **1998**, 31, 9413–9415; Gu, L.; Zhu, S.; Hrymak, A. N. *J. Polym. Sci., Part B: Polym. Phys.* **1998**, 36, 705.
- (14) Paik, H.-J.; Gaynor, S. G.; Matyjaszewski, K. *Macromol. Rapid Commun.* **1998**, 19, 47–52.
- (15) Wang, X.-S.; Armes, S. P. *Macromolecules* **2000**, 33, 6640–6647.
- (16) Wang, X. S.; Malet, F. L. G.; Armes, S. P.; Haddleton, D. M.; Perrier, S. *Macromolecules* **2001**, 34, 162–164.
- (17) Perrier, S.; Armes, S. P.; Wang, X. S.; Malet, F.; Haddleton, D. M. *J. Polym. Sci., Part A: Polym. Chem.* **2001**, 39, 1696–1707.
- (18) Hester, J. F.; Banerjee, P.; Mayes, A. M. *Macromolecules* **1999**, 32, 1643–1650.
- (19) Hester, J. F.; Mayes, A. M. In *The 1999 Membrane Technology/Separations Planning Conference Proceedings: As Presented at the Seventeenth Annual Membrane Technology/Separations Planning Conference*; Business Communications Co., Inc.: Norwalk, CT, and Newton, MA, 2000; pp 52–56.
- (20) Hester, J. F.; Mayes, A. M. *J. Membr. Sci.* **2002**, 202, 119–135.
- (21) Hester, J. F. Ph.D. Thesis. Massachusetts Institute of Technology, Cambridge, MA, 2001; p 296.
- (22) Hester, J. F.; Olugebefola, S. C.; Mayes, A. M. *J. Membr. Sci.*, in press.
- (23) Long, T. E.; Allen, R. D.; McGrath, J. E. In *Chemical Reaction on Polymer*; Benham, J. L., Kinstle, J. F., Eds.; American Chemical Society: Washington, DC, 1988; pp 258–275.
- (24) Kwon, S. K.; Choi, W. J.; Kim, Y. H.; Choi, S. K. *Bull. Korean Chem. Soc.* **1992**, 13, 479–482.
- (25) Shefer, A.; Grodzinsky, A. J.; Prime, K. L.; Busnel, J. P. *Macromolecules* **1993**, 26, 2240–2245.
- (26) Rannard, S. P.; Billingham, N. C.; Armes, S. P.; Mykytiuk, J. *Eur. Polym. J.* **1993**, 29, 407–414.
- (27) Handlin, D. L.; Thomas, E. L. *Macromolecules* **1983**, 16, 1514–1525.
- (28) Pham, Q.-T.; Petiaud, R.; Llauro, M.-F.; Waton, H. *Proton and Carbon NMR Spectra of Polymers*; John Wiley & Sons: Chichester, U.K., 1984; Vol. 3.
- (29) Pham, Q.-T.; Petiaud, R. *Proton and Carbon NMR Spectra of Polymers*; Editions SCM: Paris, 1980; Vol. 1.
- (30) Kubo, M.; Mollberg, W. C.; Padias, A. B.; Hall, H. K., Jr. *Macromolecules* **1995**, 28, 838–843.
- (31) Brandrup, J.; Immergut, E. H.; Grulke, E. A., Eds.; *Polymer Handbook*; John Wiley & Sons: New York, 1999.
- (32) Patten, T. E.; Matyjaszewski, K. *Adv. Mater.* **1998**, 10, 901–915.
- (33) Xenidou, M.; Beyer, F. L.; Hadjichristidis, N.; Gido, S. P.; Tan, N. B. *Macromolecules* **1998**, 31, 7659–7667.
- (34) Beyer, F. L.; Gido, S. P.; Buschl, C.; Iatrou, H.; Uhrig, D.; Mays, J. W.; Chang, M. Y.; Garetz, B. A.; Balsara, N. P.; Tan, N. B.; Hadjichristidis, N. *Macromolecules* **2000**, 33, 2039–2048.
- (35) Baumert, M.; Heinemann, J.; Thomann, R.; Mulhaupt, R. *Macromol. Rapid Commun.* **2000**, 21, 271–276.
- (36) Melenkevitz, J.; Muthukumar, M. *Macromolecules* **1991**, 24, 4199–4205.
- (37) Matsushita, Y.; Mori, K.; Saguchi, R.; Noda, I.; Nagasawa, M.; Chang, T.; Glinka, C.; Han, C. C. *Macromolecules* **1990**, 23, 4387–4391.
- (38) Aharoni, S. M. *Macromolecules* **1983**, 16, 1722–1728.
- (39) Sawyer, L. C.; Grubb, D. T. *Polymer Microscopy*; Chapman and Hall: London, 1987.
- (40) Jol, S.-M.; Lee, W.-S.; Ahn, B.-S.; Park, K.-Y.; Kim, K.-A.; Paeng, I.-S. R. *Polym. Bull. (Berlin)* **2000**, 44, 1–8.
- (41) Zhang, Z.; Ying, S.; Shi, Z. *Polymer* **1999**, 40, 1341–1345.
- (42) Destarac, M.; Matyjaszewski, K.; Silverman, E. *Macromolecules* **2000**, 33, 4613–4615.
- (43) Holmberg, S.; Holmlund, P.; Wilen, C.-E.; Kallio, T.; Sundholm, G.; Sundholm, F. *J. Polym. Sci., Part A: Polym. Chem.* **2002**, 40, 591–600.
- (44) Shipp, D. A.; Wang, J.-L.; Matyjaszewski, K. *Macromolecules* **1998**, 31, 8005–8008.

MA0122270